A new approach to improve mechanical properties and durability of low-density oil well cement composite reinforced by cellulose fibres in microstructural scale

Cheng, X. W., Khorami, M., Shi, Y., Liu, K. Q., Guo, X. Y., Austin, S. & Saidani, M.

DOI 10.1016/j.conbuildmat.2018.05.134
ISSN 0950-0618
ESSN 1879-0526

Publisher: Elsevier

A new approach to improve mechanical properties and durability of low-density oil well cement composite reinforced by cellulose fibres in microstructural scale.

X.W. Cheng [a,b] ,Morteza Khorami*[c], Y. Shi[a,b], K.Q. Liu[a,b], X.Y. Guo[a,b], , Stephen Austin[c] , Messaoud Saidani[c]

[a] *State Key Laboratory of Oil and Gas Reservoir Geology and Exploitation, Southwest Petroleum University, Chengdu, China*

[b] *School of Material Science and Engineering, Southwest Petroleum University, Chengdu, China*

[c] *School of Energy, Construction & Environment, Faculty of Engineering, Environment & Computing, Sir John Laing Building, Coventry University, Coventry, CV1 2HF*

**Corresponding Author:*

morteza.khorami@coventry.ac.uk and mrz_khorrami@yahoo.com

Highlight (each bullet point maximum 85 characters)

- *Cellulose fibres can improve mechanical properties of low-density oil well cement*
- *Silica fume has a positive effect on fresh and hardened properties of the composite*
- *Using both silica fume and cellulose fibres can improve the strength and durability*

Keywords: Low density, oil well cement composite, Cellulose fibre, Silica Fume, mechanical properties, Cement Composite Microstructure, Durability

In this research, a new approach was carried out to investigate the effect of incorporating cellulose fibres and silica fume into low-density oil well cement. Mechanical properties, durability and microstructure of the specimens were studied through various tests including; triaxial, flexural, tensile and compressive strength, cement sheath equivalent, permeability, mercury intrusion Porosimetry, ATR-FTIR analysis, degree of hydration and scanning electron microscopy. Twelve groups of the fibre-cement composite, with different amounts of silica fume and fibre content, were made and tested. The results show that the best performance belongs to the specimen reinforced by 8% fibre content and 15% silica fume in terms of mechanical properties and durability.

1. Introduction

Cementing is a key step in the construction of oil and gas well, which plays an important role in reinforcing well wall and sealing layers of oil and gas [1]. The success of cementing is the basis of the subsequent drilling process. In the cementing process, the cement paste is injected into the annular space between the casings and forms a cement sheath after a certain period of time. The cement sheath can effectively protect and support the casing and seal the layers of oil and water around the wellbore [2]. The use of ordinary Portland cement is not suggested for interlayer seal due to brittle failure if it is subjected to external forces. This can cause severe oil, gas and water channelling phenomena, the wastage of oil and gas resources, as well as environmental impacts such as groundwater pollution, gas channelling and overflow of fluid to the surface [3]. Therefore, it is important to maintain the integrity of the underground cement sheath to ensure the normal oil and gas production and extend the operational life of oil and gas wells [4].

* Corresponding author.
E-mail addresses: mrz_khorrami@yahoo.com

To improve brittleness, low deformation capacity and high shrinkage, a broad range of organic and inorganic products such as latex, whiskers and elastic particles have been suggested[5,6].

In addition, several common modifying fibres have been used widely including polypropylene fibre, steel fibre, polyvinyl fibre [7], polyacetal fibre [8], steel fibres [9] and carbon fibres [10]. These fibres have their own limitations such as length, diameter, aspect ratio, bonding with the fibre-cement interfacial zone, density, poor consistency with cement matrix, etc.

Compatibility of different types of polymeric and cellulose fibres in terms of durability and strength have already been studied by many researchers. The results of the carried out study showed that the cement composite reinforced by cellulose fibres could fulfil most of the required characteristics not only for durability purposes but also improving bearing capacity and toughness.[11-13].

Morteza et al studied a broad range of fibre content from 1% to 14% in increments of 1% on the flexural performance of Fibre Cement Composite (FCC). They showed that the flexural strength of FCC reinforced by 8% cellulose fibres is higher than other groups. However, they concluded with increasing fibre content, fracture toughness increases [14]. In addition, other research has [12,15-17] studied the effect of various cellulose fibres on mechanical and physical properties of FCC. They identified that polypropylene, acrylic and glass fibres could be used to improve the bearing capacity of the composite if only mixed with cellulose fibres. They showed that the flexural strength and toughness of FCC could be improved by more than 50% when the appropriate fibre content is used.

Many studies showed that Cellulose fibres (CFs) are susceptible in alkaline media. High alkaline environment, resulted from cement hydration, can reduce the durability of FCC due to dissolve lignin of CFs. To overcome this problem, the results of the carried out research showed that silica fume can reduce the alkalinity of the matrix through a chemical reaction within silica fume and calcium hydroxide which is one of the hydration products.[14,17].

With the continuous development of oil and gas exploitation to low voltage leakage, easy stratigraphic, cementing with conventional density slurry of 1.88g/cm^3 can cause leakage in wells. To overcome this problem, low-density cement slurry has been suggested [18]. Low-density cement not only can reduce the liquid column pressure, resulting in avoiding leakage, but also has a positive effect on reducing the pollution caused by setting time, which is important for reservoir protection.

Commonly used low-density cement paste system is divided into three categories including:

- By using fly ash [19], bentonite [20] and other types of ultra-fine power [21] such as a mitigating agent. Most of these mitigating agents are based on a water-absorbing component, which mainly reduces the density to 1.40 - 1.60 g/cm^3 by increasing the water-cement ratio in the slurry.
- By using lighter materials such as hard asphalt, floating beads or ceramics balls [22]. This method could produce the slurry with a lower density ranging from 1.30-1.60 g/cm^3.
- By using foam cement which uses gas as a relief compound. The density of this type of slurry is affected by the density of base grout, the inflating capacity and the pressure at the bottom. The density of this product would be as low as 0.7 g/cm^3 in low depth to around 1.30g/cm^3 in deep wells [23].

Floating beads, which are used in the production of low-density slurry, have attracted the attention of researchers in cementing technologies. However, some research works [24] focused on the presence of hollow spheres which can weaken the elastic deformation and have a negative effect on crack propagation. Low-density cement sheath plays an important role in the subsequent production process, resulting in a complex alternating load and cause the stress

changes in cement sheath. It could form cracks and holes in the inner and the surface of cement sheath when the stress exceeds. This may lead to total failure and destruction of the integrity of cement sheath [25]. So, in this research, an attempt has been made to improve this characteristic to ensure long-term performance for sealing layers.

In this research, the effects of CFs and silica fume on physical, mechanical and durability of low-density oil well cement are studied. In addition to mechanical tests to determine the bearing capacity of FCC, permeability and porosity of the specimens were investigated by mercury intrusion. To study microstructural behaviours of fibres and composite, XPS, FTIR and SEM were carried out.

Although some scholars have already studied the application of cellulose fibres in oil well cement, they mainly focused on conventional density for the cement composite. The authors did not find any study on low-density oil well cement composite incorporated by cellulose fibres. In addition, a new approach that has been utilised in this research is to study macro and microstructures of the ingredients and the specimens through a broad range of tests simulating the actual downhole conditions.

2. Experimental Procedure

2.1 Materials

The materials used in this research include:

- Cement: Class G high sulphate-resistant oil well cement was manufactured by Jiahua special Cement Co., Ltd., Sichuan, China. The chemical composition (shown in table 1) and properties of cement are in accordance with API specification RP-10A.
- Water: Potable water was used to prepare the specimen.
- Floating beads: These micro spherical shape materials have been produced by 3M Co., Ltd., USA. These materials are lightweight, have a high-temperature resistance and chemical stability. It was used as a lightening agent in the experiment.
- Micro silica fume: It was provided by Omax Co., Ltd., China. In some specimens, micro silica was replaced with 15% of cement weight. Particle size distribution and its characteristics have been depicted in Fig1 and table 2.
- Cellulose fibres: The CFS were manufactured by Regal Co., Ltd., China. The characteristics of CFS are summarised in table 3.

- **Table 1**; Chemical composition of the cement

Constituent	MgO	SO_3	R_2O	C_3S	C_2S	$2C_3A+C_4AF$	Loss
%wt	1.42	2.05	0.44	58.48	2.47	18.48	1.30

- **Table 2**; Characteristics of used Micro silica

Colour	Grey
Specific gravity	2.34
Solubility	Insoluble
Bulk density	618kg/m^3
Silicon dioxide (SiO_2) (%)	94%
Moisture content (%)	1.4%
Oversize percent retained on 45-μm (325 sieve)	0.49
Specific surface	18m^2/g

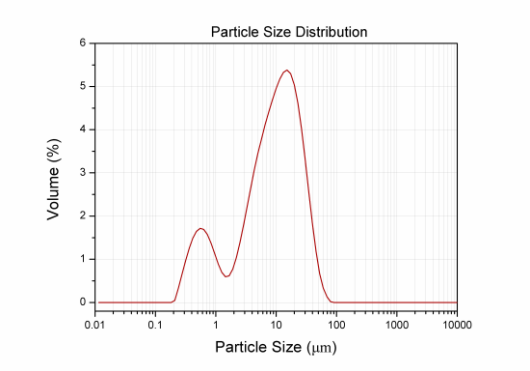

Fig. 1. The particle size distribution test for micro silica

As seen, the size of micro silica power is largely smaller than cement particles (i.e. 75μm).

Table 3; characteristics of cellulose fibres

Fibre properties	Parameter
Tensile strength (MPa)	500-1000
Average length (mm)	2-3
Diameter (μ m)	15-20
Elastic Modulus(GPa)	8-10
Specific surface area (cm^2/g)	20000-30000

The ingredients for making the specimens include; cement, water, and CFs. They were mixed together to form an aqueous slurry. To simulate the lab specimens with oil-well cementing in the field, the CFS content was designed to avoid the increase of flow frictional pressure. The mixing procedure was according to the API RP 10B-2 standard [26] and began with a pre-mixture of cement, floating beads and micro silica thoroughly to form a uniform mix.

To ensure uniformity in fibre distribution, CFs and water were mixed together in a blender at speed of 4000±250 r/min for two minutes. Then other ingredients were added accordingly in a slot of 15 seconds for each one. When the last ingredient was added, the blender mixed all materials for 30 seconds at the speed of 12000±250 r/min.

In real conditions such as downhole service situation, oil well cement must keep its consistency and productivity in high temperature and high pressure when it is used in drilling operations. To simulate those conditions, curing the specimens was done in autoclave chamber which has high temperature and pressure.

2.2 Mix design

The mix proportions of CFS-cement slurry were designed to investigate the effect of fibre content and silica fume on strength characteristics of the specimens (table 4). A broad range of CFS content was incorporated into the mixer along with water and cementitious binder to form an aqueous slurry. As seen in table 4, in some groups Micro silica was replaced with 15% weight of cement. The water-cement ratio was constant (0.44) for all groups. As seen in table 4, a control mix with neat cement was also prepared to compare the results.

Table 4 Mix proportion of the specimens

Mix design code	Cement (%)	Water (%)	Floating beads (%)	Micro silica (%)	CFS (%)
Reference (Control)	100	44	25	—	—
(C2)	100	44	25	—	2
(C2M15)	85	44	25	15	2
(C4)*	100	44	25	—	4
(C4M15)*	85	44	25	15	4
(C6)	100	44	25	—	6
(C6M15)	85	44	25	15	6
(C8)	100	44	25	—	8
(C8M15)	85	44	25	15	8
(C10)	100	44	25	—	10
(C10M15)	85	44	25	15	10

*Note: The code chosen for each group show the mix content. For instance, C4 means specimens of this group were reinforced by 4% Cellulose fibres. Similarly, C4M15 means specimens were reinforced by 4% Cellulose fibres and 15% Micro silica was replaced for the cement. The percentage mentioned in table 4 is the percentage of materials to the cement weight.

The reasons for choosing 15% silica fume as a replacement for the cement are associated with the following approaches;

- Close-packing theory deals with a dense arrangement of similar spheres in an infinite matrix to gain the highest density. Based on this theory for regular packings with two or three sized spheres, the maximum fraction could be around 80% [27]. Generalizing this concept to hydrated cement product can give a rough idea that the highest incorporation silica fume into the cement matrix could be around 20%.
- To find the appropriate silica fume content, three groups of mixes were designed based on a constant percentage of 4% cellulose fibres and different percentage (i.e. 10%, 15%, and 20%) of silica fume as the cement replacement. The results showed that 15% could lead to better characteristics of the specimens. Hence, only the results of 15% have been used for this paper.

2.3 Functional groups test of CFS

The functional group tests on cellulose fibres were carried out by an Attenuated Total Reflection Fourier Transform Infrared (ATR-FTIR) through a spectroscopic analysis accessory spectrometer (Thermo Fisher Scientific, USA). Scans were performed on the spectral range 3900-400 cm^{-1}, with a resolution of $2cm^{-1}$. Samples prepared for the FTIR were the same weight and dispersed in the matrix of KBr (200 mg KBr for each sample). The specimens were then consolidated with the compression of the sheet with minimum stress.

X-ray photoelectron spectra (XPS) of CFS were obtained by a Physical Electronics PHI Quantum 2000 instrument equipped with a monochromatic Al *K* α X-ray source and operated at 25 W with a combination of electron flood gun and ion bombarding for charge compensation. The take-off angle was 45° in relation to the sample surface. The analysed area was 500×400μm.

2.4 Mechanical characteristics

The bearing capacity of the specimens were determined through four tests including, flexural, tensile, compression and triaxial tests.

Flexural strength was carried out under a three-point load system by a universal material testing machine according to BS EN 12467: 2004. There were three specimens in each group subjected to a flexural load to failure point, which must occur between 30 and 60 seconds of loading time.

Tensile strength was done through a Brazilian splitting test based on the GB5001 standard test method on cylindrical specimens, the dimensions were 50 mm height and 25mm diameter.

Compressive strength test was conducted at a load rate of 1200±100 N per second by using a TYE-300B electronic controlled hydraulic testing machine (Wuxi Jianyi Instrument & Machinery Co., Ltd., China) with a capacity of 200KN according to API RP 10B-2 on the 50mm cubes.

A triaxial test was carried out to simulate the performance of the cement composite under high temperature and pressure when it is injected into the oil well. Due to the lack of standard tests to determine the triaxial strength of oil-well cement, the tests were performed according to ASTM D4767-2011 Standard Test Method for Consolidated Undrained Triaxial Compression Test for Cohesive Soils. The cylindrical samples of 25.4 mm diameter and 50.8 mm height were subjected to confining pressure of 20 MPa and a constant loading rate of 2 kN/min, as well as a maximum cyclic loading of 16 kN at a temperature of 60℃.

2.5 Cement sheath equivalent experiment

Cement sheaths are subjected to cyclic loading, downhole pressure and temperature variation. The cement sheath equivalent experiment test is to simulate those parameters. The bearing process, which is actually equivalent to the actual cement sheath, is obtained by simulating the casing size, temperature variation and internal casing pressure.

The grout was prepared according to API RP 10B-2 before conducting the cement sheath equivalent experiment. The grout is then poured into the annulus formed by the assembled cement sheath simulated casing mould. The cement sheath is placed at a high temperature (90℃) and high pressure (20MPa) for autoclave curing. The specimens were demoulded after seven days curing. The mould used for cement sheath integrity and the autoclave curing device are shown in Fig.2 (a) and Fig.2 (b).

The cement wellbore is designed according to the principles of geometric similarity and stress equivalence in the cement sheath equivalent experiment. The cement well simulation device, as seen in fig.3, includes 1) the simulation casting, 2) cement sheath 3) the kettle body wall and 4) sensors. To start the test, the cured cement sheath is placed into the mould. The fluid is injected into the annular space of the mould (i.e. simulation casting) by a pump to apply the pressure on the cement sheath. The heating jacket located outside the kettle body wall provides enough heat to increase the temperature. P_0 and P_1, shown in fig.3b, are used to simulate the confining pressure and casing pressure respectively. To apply and control the pressures accurately MathCad software was deployed.

Fig. 2(a). Conservation mould of Cement sheath integrity

Fig. 2(b). Autoclave Curing device

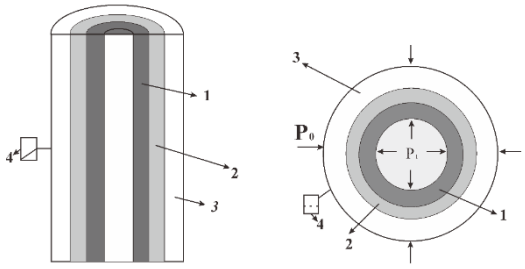

(a) (b)

Fig.3. Diagram of the wellbore simulator: (a) Front View and (b) Vertical View

1. Simulation Casing 2. Cement sheath 3. Kettle body wall 4.Sensor

2.6 Cement Permeability Test

The permeability test was carried out by using DKS-3 core permeability equipment. The schematic illustration of the porosity and permeability test is shown in Fig. 4.

This test is based on measuring the input and output pressure of gas injected into the specimen. So, firstly, the pressure regulator along with gas inlet and all the valves must be turned off. Secondly, only the gas test valve should be turned on while the check valve, liquid test valve and liquid output valve are turned off. Thirdly, by turning on the gas inlet slowly, the pressure in the regulator increases to remove any existing liquid in the pipelines. In this stage, by turning on the pressure relief valve slowly the gas can pass through the pressure relief valve to determine the permeability of the specimen, which is shown on the flow meter directly.

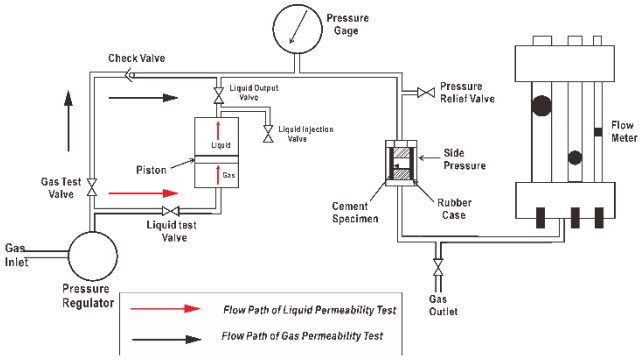

Fig. 4. Schematic illustration of permeability test

2.7 Mercury Intrusion Porosimetry

MIP analysis is applied to determine the size of pores in the specimens. Mercury Intrusion Porosimetry (MIP) was carried out by Quantachrome Poremaster with high pressures of 200 MPa. The surface tension and density of mercury are 480 mN/m and 13.53 g/cm^3 respectively. Equilibration time for both low and high pressure was the 20s. The contact

angle was 130°. To prepare the sample for this test, a small piece (about 5mm length) was cut from the specimen and dried at the temperature of 60℃for 24h.

2.8 Scanning electron microscope (SEM) analysis

The morphology and microstructure of CFS and cementitious composite have been studied by a Scanning Electron Microscope (Quanta 450, FEI, USA) at a voltage of 2000 kV. The samples have been prepared by gold coating for this test.

2.9 Thermal analysis (DTG/TGA) for Degree of Hydration (DoH)

The most commonly used test to determine DoH is thermal analysis by measuring Derivative Thermo-Gravimetric analysis (DTG) and Thermo-Gravimetric-Analysis (TGA). DTG can locate the limits associated with thermal decompositions of different phases in the paste. Simultaneously, the weight loss resulted from decompositions is measured by TGA.

The equipment used for this test is a DSC 823 TGA/SDTA85/e (METTLER TOLEDO Co., Switzerland) with a balanced accurate to 0.1mg and heating rate of 10℃/min. The reference material used for this test is α-alumina (α - Al2O3) which has already been calcined at 1500℃.The test was undertaken within a full N2 environment.

DoH is an important indicator to identify the fraction of cementitious materials in the past which has fully reacted with water. DoH is directly proportional to the amount of water that has been used for chemical bonding. By increasing the temperature of ignition from105 ºC to 1000 ºC, all water has been used for chemical bound is lost.

The philosophy of this test is based on the mass loss due to decomposition of the sample when the temperature increases from boiling temperature of 105°C to a maximum of 1000°C in which the whole of chemically bound water used for hydration reaction is lost.

3. Results and discussion

3.1 Functional groups of CFS

3.1.1 X-ray photoelectron spectra (XPS) analysis

XPS, which is the most common analytical technique for analysing the samples, was used to identify the functional groups on the CFS surface. The typical whole spectrum of CFS surface is shown in Fig. 5. The whole spectrum, illustrated in Fig.5 (a), shows that CFS surface consists mainly of carbon and oxygen (hydrogen is not detectable by XPS). As shown in fig.5, on the surface of CFS the first orbital-free electrons on both carbon and oxygen atoms undergo a transition when irradiated with X-ray.

O1s peak spectrum and C1s peak spectrum are shown in Fig. 5 (b) and (c) respectively. As seen, the aliphatic carbon region (designated as C-C or C1) is located at 284.8eV. Ideally, cellulose might be devoid of C1 carbon due to its polysaccharide structure [28]. However, due to the presence of lignin in CFS, C1was also detected in the test. The C-O was also detected in the XPS graph, which can show the presence of functional groups in CFS.

Fig. 6. shows three common monomers of lignin, including; a) Para-hydroxy-phenyl lignin (H-lignin), b) Guaiacyl lignin (G-lignin) and c) Syringyl lignin (S-lignin), respectively. As the CFS used in the experiment were provided from a factory that uses a broad range of sources and prefers not to reveal the secret of their business, the type of wood species (e.g jute, hemp, sisal, coir, pine et al) was unknown. However, the results show that in the presence of lignin the CFs have the same functional group including; C-C and C-O [29]. As outlined, the CFs used in this research have lignin which can adversely affect the hydration process. Since lignin plays an important role in linking the individual filaments with each other, by dissolving lignin in high alkaline media, resulted from cement hydration, a degradation on flexural performance

is expected during the serviceability of Cement composite. CFs can suffer decomposition not only in early age after casting, but also could be attacked in hardened cement composite. In hardened cement composite there are some voids and pores which are formed due to different types of hydrated products such as calcium silicate hydrate (CSH gel), Ettringite and calcium hydroxide or Portlandite. When cement composite is exposed to moisture, water is sucked by capillary action into the composite and lead to dissolve calcium hydroxide which can form high alkaline media, consequently dissolving lignin and decreasing the bond in the fibre-cement interfacial surface.

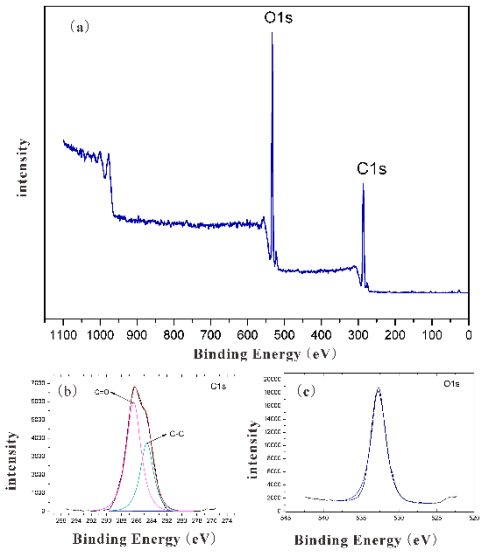

Fig. 5. XPS Spectrum of CFS: (a) whole spectrum, (b) O1s peaks spectrum and (c) C1s peaks spectrum

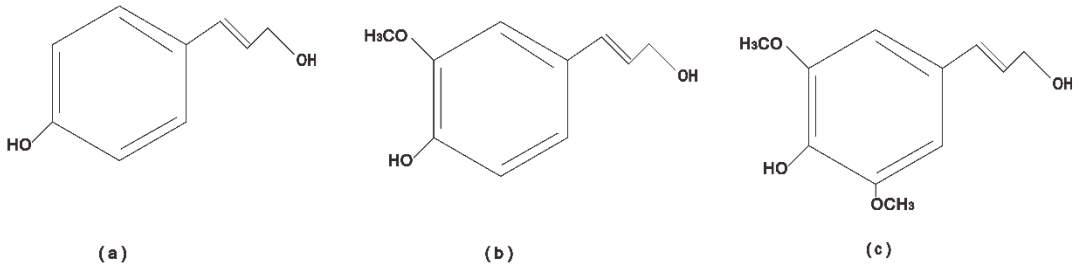

Fig. 6. The structure of the three monomers of lignin: (a) Para-hydroxy-phenyl lignin (H-lignin), (b) Guaiacyl lignin (G-lignin) and (c) Syringyl lignin (S-lignin)

3.1.2 ATR-FTIR analysis

FTIR is used to determine the main functional groups in CFs. The results of FTIR spectra are shown in Fig. 7. Bands frequency of the functional groups of lignocellulose, including cellulose, hemicellulose, and lignin can be observed in the figure.

Alkanes, aromatic groups and different functional groups including acid anhydride and alcohol are detected in CFs structure. The bands observed at 3426 cm^{-1} are related to the -OH stretches. The bands at 2905 cm^{-1} and 1379 cm^{-1} are related to $-CH_3$, which are typical of symmetric stretching of C-H bonds in hemicellulose and cellulose, respectively [30]. The bands in the range of 1638 cm^{-1} and 1449cm^{-1} belong to C=C and CH_2 symmetric stretching. C=C is related to the lignin that has already been discussed. The band at 1160cm^{-1} is attributed to C3 carbon vibrations of cellulose. The band at 1062 cm^{-1} is related to the vibration of C-O-C glycosidic linkage of the cellulose. The band observed at 1134 cm^{-1} is

associated with C-O due to the secondary alcohol, which can show the presence of the functional group of lignin, cellulose, and hemicellulose [31].

As observed in the bands' frequency of the functional groups of lignocellulose, in addition to cellulose, there is a significant amount of hemicellulose and lignin. In the cement hydration process, the filaments of cellulose fibres are attacked by high alkaline pore water existed in micro pores and could lead to crystallization of CFs. The embrittlement of the CFs can weaken the fibre-cementitious interfacial bonding [17].

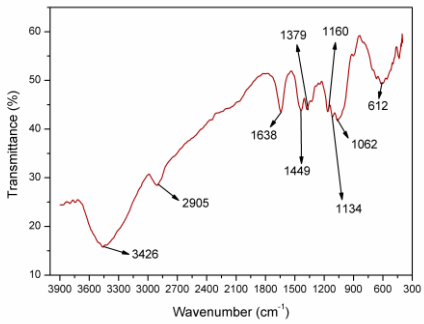

Fig. 7. FTIR spectra of the CFS

3.2 Mechanical strength Properties

3.2.1 Tensile, Flexural and Compressive strength

The effect of fibre content and micro silica content on the tensile strength and Module of Rapture (Flexural strength) and compressive strength of low-density cement composites are shown in Fig.8. In the early age of curing process, Tricalcium Silicate (C3S) of the cement reacts with water to produce Calcium silicate hydrate gel (C-S-H) and calcium hydroxide (CH). C-S-H has a fundamental role in the formation of matrix strength while CH doesn't have.

At the age beyond 7 days, Dicalcium Silicate (C2S) of the cement reacts with water and contributes to strength growth by producing C-S-H and CH. As already mentioned, silica fume was replaced for cement in some mixes. One of the important advantages of incorporating silica fume into the mix is to react with CH. CH is not been considered as a useful hydration product but it can react with silica fume to produce C-S-H.

As seen in Fig.8, with increasing fibre content, tensile strength increases. The trend of increasing tensile strength is consistent with increasing flexural strength, excluding group C2 which will be discussed later. As seen, the optimum fibre content belongs to the specimens reinforced by 8% CFs which can achieve the highest tensile and flexural strength. Similar results have already been reported by Morteza et al [14].

As outlined, only FCC reinforced by 2% CFs showed poor performance in comparison with other groups and an even weaker performance than the reference group. This weak performance is associated with non-uniform fibre distribution throughout the matrix. This has been confirmed when the cross-section of the specimens was observed after failure. Lack of uniform fibre dispersion into the matrix causes a disruption in transferring the stress within the matrix ingredients, resulting easily in cracks propagation.

By increasing fibre content from 2% to 8%, the bearing capacity increases as seen in fig.8ut when the fibre content reaches 10% a reduction in both flexural and tensile strength is observed. This could be related to the lack of hydrated cement products needed to immerse the CFs. In other words, when the amount of fibres exceeds there are not enough hydrated cement products to immerse them and some fibres are accumulated next to each other and can increase the pores, which adversely affect the bearing capacity.

The effect of replacing 15% of the cement weight by silica fume in increasing the tensile and flexural strength is observed in Fig8. The increase can be attributed to two important characteristics of silica fume. 1) Micro silica particles are extremely small and can reduce the porosity by filling the pores which can improve permeability and bearing capacity. 2) Due to the pozzolanic reaction within silica fume and calcium hydroxide, which is one of the non-desirable

hydration products, the most favourite hydration product Calcium Silicate Hydrate (CSH) is produced which can increase the strength of the composite [17]. As seen in fig 8a, with increasing the cellulose fibres, the tensile strength increases proportionally. Although the amount of increased tensile strength is not big, the rate of increasing follows a regular trend which can highlight the effect of fibre content.

As known, the cement paste is weak in taking tensile strength. This will not be improved significantly even though by replacing silica fume for the cement. In addition to filler action, the main role of silica fume in the mix is its pozzolanic action to produce hydrated cement products particularly C-S-H. Obviously, if there is an appropriate bond within the hydrated cement products and the incorporated fibres, the tensile strength will be improved. The presence of silica fume can only improve bonding within fibre-cementitious interfacial zone so, it can increase the tensile strength of the specimens indirectly.

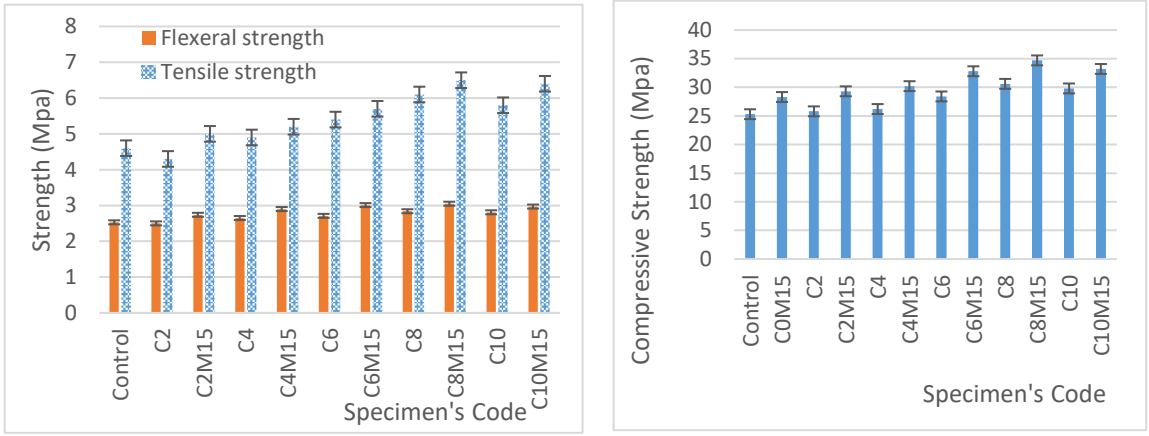

a) Tensile and Flexural strength b) Compressive strength

Fig.8 Mechanical characteristics of the specimens

The compressive strength of the specimens is shown in Fig.8b. As seen the compressive strength of the specimens incorporated 15% micro silica (e.g. C0M15) is increased compared to the reference specimens. For example, the compressive strength of C0M15 is 28.3Mpa, which is about 10% higher than reference specimens. This can highlight the effect of silica fume in increasing the compressive strength.

As illustrated, the optimum fibre content to get the maximum compressive strength belongs to 8% fibre content. These results are consistent with other carried out mechanical tests such as; tensile and flexural tests. So, most of the justifications for this behaviour could be the same as already outlined. More details particularly microstructure of the composite will be discussed in the next sections.

3.2.2 Triaxial stress-strain behaviour

Fig.9 compares the stress-strain of three significant specimens as the representative of their corresponding groups. As seen, the reference graph which belongs to the specimens made with solely cement is stiffer than others because the initial modulus of elasticity, which is based on the gradient of stress-strain, is higher than others. The second graph which belongs to the specimen reinforced by 8% CFs shows that incorporating fibres into the matrix can reduce the stiffness. This is due to the fact that CFs can increase the ductility of the specimens by a crack-bridging function, which is directly related to stress redistribution when cracks initiate over the loading process. The mechanism of crack- bridging not only improves the ductility of the specimen but can also increase the failure stress of the specimen. This means interfacial bonding within fibre cementitious materials can enhance the bearing capacity of the specimen.

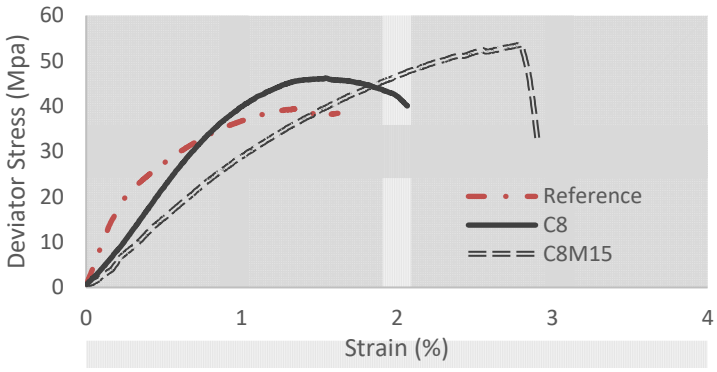

Fig. 9. Triaxial stress-strain curves of reference, C8 and C8M15

The effect of silica fume in toughness and failure stress is shown by C2M15 in fig.9. As outlined, due to pozzolanic reactivity and filler function, it was predicted to increase the failure stress and toughness. Failure stress has been increased due to a greater amount of Calcium-Silicate-Hydrate, which has been formed due to the pozzolanic reactivity of silica fume and reacts with calcium hydroxide in the hydration process. Greater toughness is associated with increasing the bonding in the fibre-cementitious interfacial zone, which is largely based on filler function of the silica fume.

3.3Fractured surface morphology

Microstructure studies of the samples including; reference, C8 and C8M15 were carried out using SEM. Fig.9a shows an overview of reference sample by illustrating the distributed bobbles resulted from floating beads which have been dispersed throughout the sample. Individual bubbles without interconnecting path between them show that the floating beads could perform their function well. In other words, as expected, floating beads can reduce the density of the sample by entering the bubbles into the matrix while it would not have an adverse effect on the permeability of the sample.

Fig 9b shows the reference sample when it was broken under failure load. The formation of cracks and mode of failure are highlighted in this figure. As seen, when the cracks initiate in loading, the bubbles resulted from floating beads cannot sustain or transfer the load and start failing consecutively. Then, the cracks link with each other and total failure occurs.

Fig.9c belongs to C8 which can illustrate a filament of CFs which have been confined by hydrated cement products. The interfacial bonding could change the mechanism of failure positively from brittle to ductile failure. However, some of the hydrated cement products such as CSH can be seen on the surface of the fibre but some parts of the fibre are free of hydrated cement products. This is associated with the size of fibre, pores, hydrated cement products and interfacial bonding. It is clear that if the fibre is immersed in hydrated cement products, the bonding in interfacial zone increases.

Fig9d and 9e show the mechanism of failure which could be either fibre pull-out or fibre snapping. When the specimen is subjected to loading, the cracks initiate when the tensile strength reaches the threshold of bearing capacity. When the cracks form, the fibres participate in the loading procedure through interfacial fibre- cementitious bonding. If the fibres have been immersed in hydrated cement products, the failure tends to be fibre snapping, whereas fibre pull-out occurs when the bonding in the fibre-cement interface is less than the tensile strength of the fibres. As seen in Fig9d, which belongs to the specimen reinforced by 2% CFs, fibre snapping is the dominant failure mechanism. As the fibre content is only 2%, the fibres have been immersed in hydrated cement products which can provide a strong bonding in the fibre-cement interface. In fig.9e, which belongs to the specimens reinforced by 8% fibres, the mechanism of failure is predominantly pull-out rather than fibre snapping which can be observed with the footprints of the fibres. When the fibre content increases, the number of CFs which can contribute to load transferring increases as well. Therefore, fibre pull-out would control the overall failure.

Fig.9f shows the microstructure of the sample which comprises of silica fume. As can be observed, silica fume could

decrease the porosity of the matrix by filling the pores, which can lead to increasing the bonding in the fibre-cement interface. In addition, due to the pozzolanic reaction of silica fume, more hydrated compounds, particularly CSH, attached to the fibre surface. Less porosity in the matrix and greater engagement within the fibre-cement interfacial zone cause a further increase in efficiency of fibre reinforcing which results in greater toughness as well as mechanical strength.

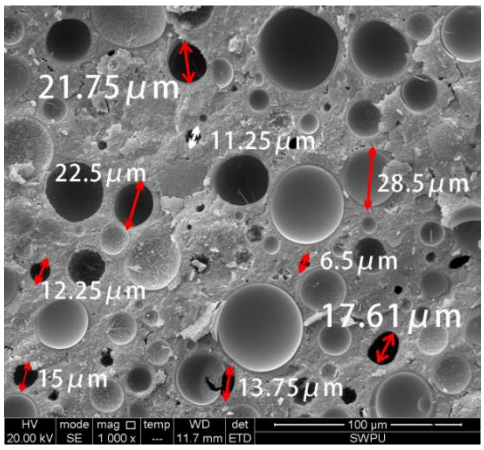

Fig.9a. an SEM of the complete reference specimen (×2000)

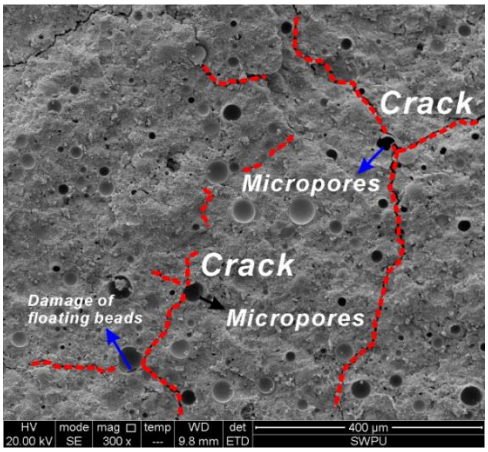

Fig.9b SEM of the damaged reference specimen (×300)

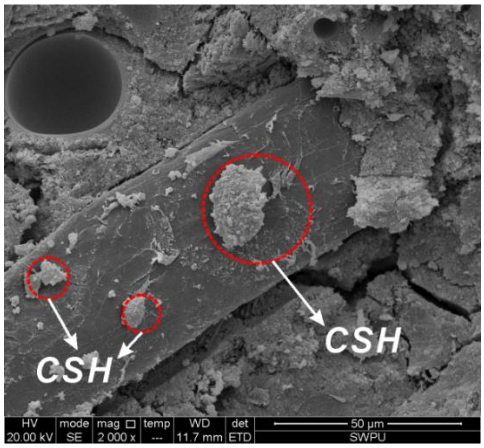

Fig.9c. Hydrated cement products distribution on CFs (×2000)

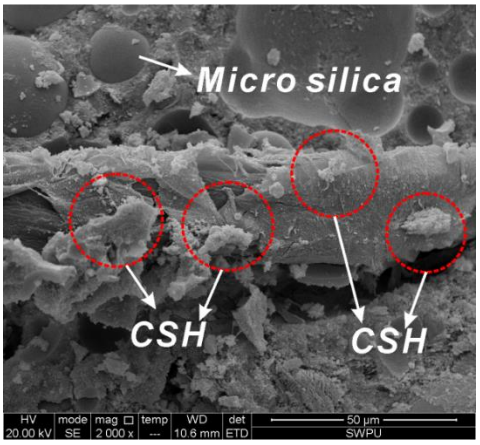

Fig.9d. Effect of Micro silica on the structure of specimen with CFs (×2000)

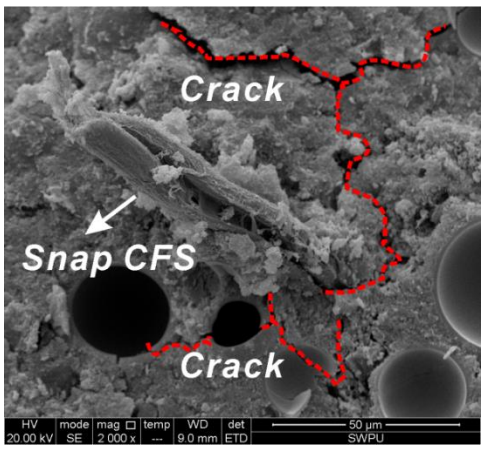

Fig.9e. Interfacial zone of CFs and hydrated cement product for C2 (×1000)

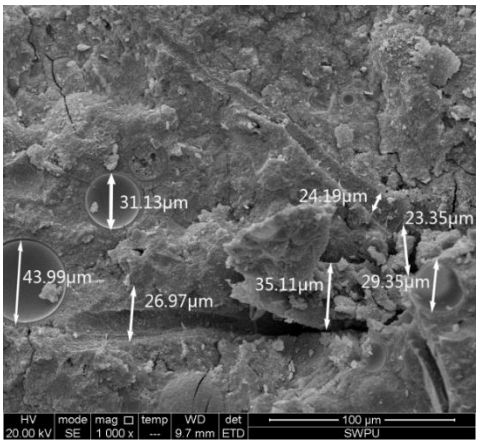

Fig.9f. Interfacial zone of fibres and hydrated cement products for C8

3.4 Cement sheath equivalent experiment analysis

The results of the Cement sheath equivalent experiment which was taken under a confinement pressure of 30 MPa

are shown in table 5. As seen, the reference cement sheath could prevent the gas migration when the casting pressure increased from 25MPa to 55MPs and remained for 5 minutes. However, by increasing the casting pressure to 65MPa the reference cement sheath could only resist for 1 minute and then the structure of the specimen was comprised, losing isolation performance and gas migration occurred.

The complete cement sheath and compromised cement sheath are shown in Fig. 10(a) and (b).

Incorporating fibres into the cement sheath could improve its bearing capacity as shown for C8 in table 5. As tabulated, 8% fibre content could increase casting pressure up to 75MPa for 5 minutes but when the pressure reached 85MPa, it could still resist for one minute before losing its structure and place the gas migration taking place. This shows that incorporation of fibres could increase the integrity of the bearing capacity of the specimen by modifying the load transmission within the matrix components.

Incorporating both silica fume and CFs could increase the bearing capacity cement sheath dramatically as seen for C8M15. As outlined in table 5, casting pressure applied on C8M15 was increased to 95 MPa with a duration time of 5 minutes. However, whilst the casting pressure was being decreased to 75MPa the sample lost its integrity and could only resist for one minute before gas migration took place.

This improvement in bearing capacity is associated with both filler action and pozzolanic reactivity of silica fume. Filler action could predominantly improve the porosity of the matrix, which has a positive effect on gas migration. Pozzolanic reactivity of silica fume could increase CSH, which has the most important role in increasing the strength of hardened cement.

Table 5;Test results of the Reference, C8 and C8M15 in the wellbore simulator under 30 MPa (temp: 50℃)

Loading conditions	Confinement pressure(MPa)	Casing pressure(MPa)	Equivalent pressure(MPa)	Duration Time (min)		
				Reference	C8	C8M15
1	30	25	10	5	5	5
2	30	35	18	5	5	5
3	30	45	27	5	5	5
4	30	55	35	5	5	5
5	30	65	44	1	5	5
6	30	75	52	/	5	5
7	30	85	60	/	1	5
7	30	95	68	/	/	5
8	30	85	60	/	/	5
9	30	75	52	/	/	1
10	30	65	44	/	/	/

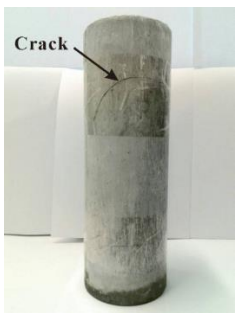

a b

Fig. 10. The images of cement sheath: (a) Complete cement sheath and (b) Compromised cement sheath

3.5 Cement Permeability Test and Mercury intrusion Porosimetry analysis

The results of permeability for three specimens including reference, C8 and C8M15 are tabulated in table 6. This test can determine the important factors associated with capillary pores and microvoids such as total pore areas, average pore diameter, porosity and permeability. It is well known that for fibre cement composite, the higher permeability, the less durability. High propriety and permeability can adversely affect most of the cement composites such as mechanical properties, water absorption and durability. Comparing the tabulated date for samples show that the reference sample has low porosity and permeability in comparison with C8. It means incorporating fibres into the mix would increase the capillary pores which were predictable due to the intrinsic characteristics of cellulose fibres. But, as seen by the introduction of silica fume into the mix, all permeability factors including; pore diameter, porosity, and total pore area are reduced dramatically due to filler action and pozzolanic reactivity of silica fume. This outcome is consistent with the observation and justifications which have already been discussed in the SEM section.

Table 6; Cement permeability test and Mercury intrusion Porosimetry for the specimens

Mercury intrusion Porosimetry data	Reference	C8	C8M15
Total intrusion volume (mg/L)	0.4594	0.4237	0.1477
Total pore area (m^2/g)	42.647	50.005	20.873
Median Pore Diameter- Volume (µm)	25.8	37.5	22.7
Average Pore Diameter-4 V/A (µm)	23.0	34.3	19.7
Porosity (%)	39.6929	44.2429	24.2989
Permeability (mD)	0.049	0.054	0.040

3.6 Thermal analysis (DTG/TGA) for Degree of Hydration (DoH)

The decomposition of hydrated cement products is mainly divided into three stages as shown in fig.11. It should be noted that only the free water (Not chemically bound water) is evaporated when the temperature is between 25°C and 105°C.

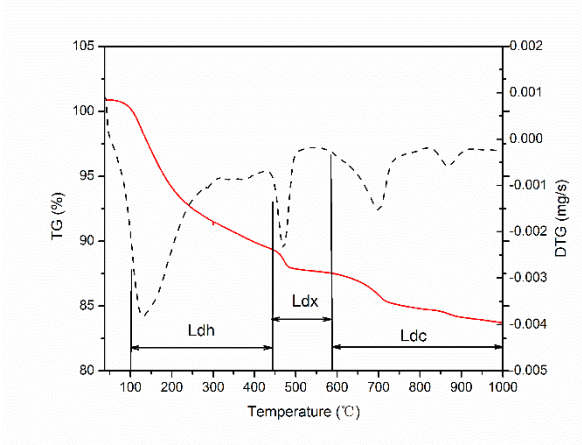

Fig 11. Generic DTA-TG curves of cement paste

As seen the chemically bound water is lost in three stages as follows;

- Ldh: in the first stage of decomposition due to dehydration of CSH when the temperature ranging from105-440°C.
- Ldx: in the second stage of decomposition due to dehydroxylation of CH (Ca(OH)2 or Portlandite) when the temperature ranging from 440-580°C.

- Ldc: in the third stage of decomposition due to decarbonation of CaCO3 when the temperature ranging from 580-1000°C

In this research, the method used for DoH is based on Method of Bhatty's Equation [32] and free CH analysis [33,34]. Bhatty pointed out that the degree of hydration of the cement matrix satisfies the following formula：

Wb= Ldh+ Ldx+ 0.41 (Ldc) Eq (1)

α= Wb/0.24 Eq (2)

where, Ldh， Ldx and Ldc represent the process of dehydration of CSH, dehydroxylation of Calcium Hydroxide and decarbonation of Calcium Carbonate in DTG-TGA curves, respectively. The value of 0.41 represents a coefficient to consider the bound water derived from carbonated portlandite. Wb is the chemically bound water content at time t. Wb, Ldh, Ldx, Ldc are expressed in mass per unit and α is the degree of hydration and expressed in percentage.

In Eq. (2), the value 0.24 is the chemically bound water content at an infinite time (Wb) estimated from the theoretical stoichiometry of cement (Bogue's formulae) that has been used by Bhatty [32].

Eq 3 has been used by several authors in order to evaluate the free CH [33,34]

Free CH= 4.11 Ldx + 1.68Ldc Eq (3)

The thermal analysis for the selected specimens is shown in Fig 12 along with the main parameters tabulated in table7. As seen in table 7, the degree of hydration (α) of the specimens has increased from 55.2% for reference specimens to 58.8% for C0M15. Introduction of 15% silica fume to reference specimens could increase the degree of hydration to 3.6% whereas free CH content reduces from 15.9% to 14%. This can highlight the pozzolanic reactivity of silica fume which can enhance the DoH by increasing CSH content and reducing the calcium hydroxide content. As already outlined, CSH has the fundamental influence on mechanical properties of the hardened cement past.

The degree of hydration (α) for C8 is 54.03% which is slightly less than 55.21% of the reference specimen. This is associated with two characteristics of the cellulose fibres including; 1) presence of lignin and 2) large specific surface area and strong hydrophilic property.

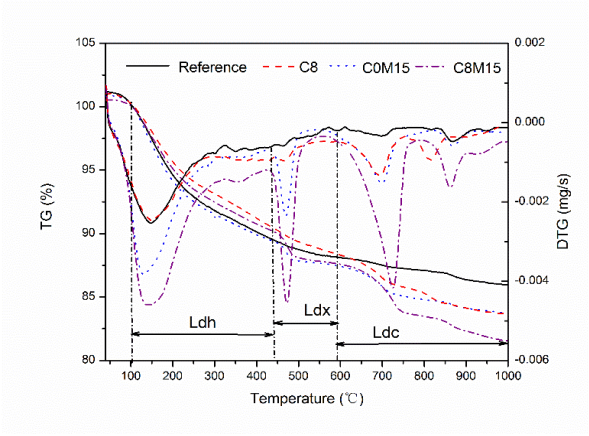

Fig.12. DTA-TG Analysis of four specimens

Table 7. Relative values from DTA-TG test in paste samples

Specimens	Ldh(%)	Ldx(%)	LdC(%)	WB(%)	α(%)	Free CH(%)
Reference	9.38	1.78	5.1	13.25	55.21	15.88
C0M15	10.7	1.98	3.5	14.12	58.81	14.02
C8	9.25	1.75	4.8	12.97	54.03	15.26
C8M15	10.3	1.9	3.95	13.82	57.58	14.45

Lignin comprises of complex polymer with high molecular weight and contains various sugar units. Sugars even in very low concentration can retard the setting time of the cement as well as a reduction in the strength of the matrix [11,15] . This is due to this fact that lignin can be solved in alkali media resulted from hydration process and adversely affects the exothermic hydration characteristics of Portland cement [14,16,35].

High specific surface areas and strong hydrophilic character of cellulose fibres cause a significant amount of cement particles tend to adhere to CFs where the concentration of lignin is relatively higher than other areas of the matrix. This can adversely affect the hydration process and consequently a reduction in the degree of hydration.

Although the introduction of CFs into the matrix has a slightly negative effect on the hydration process, it could improve mechanical properties of the matrix by bridging the cracks of cement matrix [14,17] and transfer the stresses as already discussed in SEM section.

The amount of free CH as illustrated in table 7 for C8 and reference specimens has not been changed significantly.

The degree of hydration α for C8M15 is increased to 57.58% compared with the reference specimen (α = 55.21%). Comparing α for C8M15 with C8 and C0M15 shows that 57.58% is between 54.03% and 58.81%. This means the introduction of silica fume has improved the hydration process even though the cellulose fibres has already reduced slightly the degree of hydration. In other words, this results showed that the influence of silica fume in improving the hydration reactions is greater than the effect of cellulose fibres in the weakening of hydration reactions. Therefore, as already discussed in mechanical properties section, C8M15 could exhibit the highest mechanical properties which have been resulted from the interaction of cellulose fibres as an inhibitor for crack propagation, silica fume as filler and pozzolanic materials to improve the bonding in interfacial zone, and hydrated cement products as a binder.

4 Conclusion

In this research, an attempt was made to investigate the effect of silica fume and fibre content on strength and durability of low-density oil well cement composite. The results show that cellulose fibres can improve the strength of the composite but has an adverse effect on durability parameters such as permeability and porosity. In addition, the presence of lignin in cellulose fibres can reduce the lifetime of the composite due to degradation of the fibres in high alkaline media resulted from cement hydration. To overcome on the aforementioned problems an approach focused on the use of silica fume due to its filler action and pozzolanic reactivity. The results show that by replacing 15% silica fume for the cement into the specimens reinforced by 8% fibre content, both mechanical strength durability of the cement composite was improved.

Acknowledgements

The authors are grateful for the support provided by the National Key R&D Program of China (2016YFB0303600). The authors also would like to thank Advanced Cementing Materials Research Centre of SWPU for the kind assistance in laboratory testing.

References

[1] Cheng X, Mei K, Li Z, Zhang X, Guo X. Research on the Interface Structure during Unidirectional Corrosion for Oil-Well Cement in H2S Based on Computed Tomography Technology. Ind Eng Chem Res 2016;55:10889-95.

[2] Cheng X, Jiao S, Zhang H, Li Z, Guo X. Investigation of Cement Slurry with Alkali Treated Sisal Fibers for Lost Circulation. Asian Journal of Chemistry 2012;24:2191.

[3] Kiran R, Teodoriu C, Dadmohammadi Y, Nygaard R, Wood D, Mokhtari M et al. Identification and evaluation of well integrity and causes of failure of well integrity barriers (A review). Journal of Natural Gas Science and Engineering 2017;45:511-26.

[4] Li Z, Zhang K, Guo X, Liu J, Cheng X, Du J. Study of the failure mechanisms of a cement sheath based on an equivalent physical experiment. Journal of Natural Gas Science and Engineering 2016;31:331-9.

[5] Wang M, Chung D. Understanding the increase of the electric permittivity of cement caused by latex addition. Composites Part B: Engineering 2018;134:177-85.

[6] Li Y, Wang P, Wang Z. Evaluation of elastic modulus of cement paste corroded in bring solution with advanced homogenization method. Constr Build Mater 2017;157:600-9.

[7] Qiu J, Lim XN, Yang E. Fatigue-induced in-situ strength deterioration of micro-polyvinyl alcohol (PVA) fiber in cement matrix. Cement and Concrete Composites 2017;82:128-36.

[8] Yang T, Han E, Wang X, Wu D. Surface decoration of polyimide fiber with carbon nanotubes and its application for mechanical enhancement of phosphoric acid-based geopolymers. Appl Surf Sci 2017;416:200-12.

[9] Beglarigale A. Electrochemical corrosion monitoring of steel fiber embedded in cement based composites. Cement and Concrete Composites 2017;83:427-46.

[10] Chen Z, Zhou X, Wang X, Guo P. Mechanical behavior of multilayer GO carbon-fiber cement composites. Constr Build Mater 2018;159:205-12.

[11] Khorami M, Sobhani J. An experimental study on the flexural performance of agro-waste cement composite boards. Int J Civ Eng 2013;11:207-16.

[12] Khorami M, Ganjian E. Comparing flexural behaviour of fibre–cement composites reinforced bagasse: Wheat and eucalyptus. Constr Build Mater 2011;25:3661-7.

[13] Jarabo R, Monte MC, Blanco A, Negro C, Tijero J. Characterisation of agricultural residues used as a source of fibres for fibre-cement production. Industrial Crops and Products 2012;36:14-21.

[14] Khorami M, Ganjian E. The effect of limestone powder, silica fume and fibre content on flexural behaviour of cement composite reinforced by waste Kraft pulp. Constr Build Mater 2013;46:142-9.

[15] Ganjian E, Khorami M. Application of Kraft and Acrylic Fibres to Replace Asbestos in Composite Cement Board. 2008:52-61.

[16] Khorami M, Ganjian E, Srivastav A. Feasibility Study on Production of Fiber Cement Board Using Waste Kraft Pulp in Corporation with Polypropylene and Acrylic Fibers. Materials Today: Proceedings 2016;3:376-80.

[17] Khorami M, Ganjian E, Mortazavi A, Saidani M, Olubanwo A, Gand A. Utilisation of waste cardboard and Nano silica fume in the production of fibre cement board reinforced by glass fibres. Constr Build Mater 2017;152:746-55.

[18] Bu Y, Song W, Wang M, He Y. The improvement of cementation quality rating method based on compressive strength for low density cement system. Procedia Engineering 2011;18:289-94.

[19] Gao Y, Hu C, Zhang Y, Li Z, Pan J. Investigation on microstructure and microstructural elastic properties of mortar incorporating fly ash. Cement and Concrete Composites 2017.

[20] Sha F, Li S, Liu R, Li Z, Zhang Q. Experimental study on performance of cement-based grouts admixed with fly ash, bentonite, superplasticizer and water glass. Constr Build Mater 2018;161:282-91.

[21] Oruji S, Brake NA, Nalluri L, Guduru RK. Strength activity and microstructure of blended ultra-fine coal bottom ash-cement mortar. Constr Build Mater 2017;153:317-26.

[22] Li H, Xu D, Feng S, Shang B. Microstructure and performance of fly ash micro-beads in cementitious material system. Constr Build Mater 2014;52:422-7.

[23] Glosser D, Kutchko B, Benge G, Crandall D, Ley M. Relationship between operational variables, fundamental physics and foamed cement properties in lab and field generated foamed cement slurries. Journal of Petroleum Science and Engineering 2016;145:66-76.

[24] Li Z, Sun J, Luo P, Lin L, Deng Z, Guo X. Research on the law of mechanical damage-induced deformation of cement sheaths of a gas storage well. Journal of Natural Gas Science and Engineering 2017;43:48-57.

[25] Liu H, Bu Y, Nazari A, Sanjayan JG, Shen Z. Low elastic modulus and expansive well cement system: The application of gypsum microsphere. Constr Build Mater 2016;106:27-34.

[26] API R. 10B-2, Recommended Practice for Testing Well Cements. 2013. Washington, DC: API.

[27] Stroeven P, He H. Packing of non-spherical aggregate particles by DEM. 2013.

[28] Johansson L, Campbell J, Koljonen K, Stenius P. Evaluation of surface lignin on cellulose fibers with XPS. Appl Surf Sci 1999;144:92-5.

[29] DeLucia NA, Das N, Overa S, Paul A, Vannucci AK. Low temperature selective hydrodeoxygenation of model lignin monomers from a homogeneous palladium catalyst. Catalysis Today 2018;302:146-50.

[30] Jabli M, Tka N, Ramzi K, Saleh TA. Physicochemical characteristics and dyeing properties of lignin-cellulosic fibers derived from Nerium oleander. Journal of Molecular Liquids 2018;249:1138-44.

[31] Wang W, Liang T, Bai H, Dong W, Liu X. All cellulose composites based on cellulose diacetate and nanofibrillated cellulose prepared by alkali treatment. Carbohydr Polym 2018;179:297-304.

[32] Bhatty JI. Hydration versus strength in a portland cement developed from domestic mineral wastes—a comparative study. Thermochimica acta 1986;106:93-103.

[33] Monteagudo S, Moragues A, Gálvez J, Casati M, Reyes E. The degree of hydration assessment of blended cement pastes by differential thermal and thermogravimetric analysis. Morphological evolution of the solid phases. Thermochimica Acta 2014;592:37-51.

[34] Deboucha W, Leklou N, Khelidj A, Oudjit MN. Hydration development of mineral additives blended cement using thermogravimetric analysis (TGA): Methodology of calculating the degree of hydration. Constr Build Mater 2017;146:687-701.

[35] Morteza Khorami , Eshmaiel Ganjian. Improvement of Flexural Performance of Fibre Cements Composite Board through Fibre Impregnation. Fourth International Conference on Sustainable Construction Materials and Technologies, SCMT4, Las Vegas, USA, 2016;2:693-9.